Competition of superconductivity and magnetism in $MoSr_2R_{1.5}Ce_{0.5}Cu_2O_{10-\delta}$ (R = rare-earth)

I. Felner and E. Galstyan
Racah Institute of Physics, The Hebrew University, Jerusalem, 91904, Israel
(Received 15 April 2003; published 21 August 2003)

We have investigated the $MoSr_2R_{1.5}Ce_{0.5}Cu_2O_{10-\delta}$ (Mo-1222R, R = rare earth) system by several complementary experimental techniques. In contrast to the isostructural $RuSr_2R_{1.5}Ce_{0.5}Cu_2O_{10-\delta}$ (Ru-1222) system, in which superconductivity (SC) in the CuO_2 planes and *weak* ferromagnetism in the Ru sublattice coexists, in Mo-1222, displays a competition between the two states, namely, SC vanishes when the magnetic order sets in. The contraction in the R elements leads to a change of the physical states. The light R ions (Pr and Nd) are paramagnetic down to 5 K, whereas the middle R ions (Sm and Eu) are SC at T_c 18–23 K, respectively. The SC charge carriers originate from the CuO_2 planes, and annealing under oxygen pressures does not affect T_c. A simple model for the SC state is proposed. For the heavy R elements Ho-Lu and Y, the pentavalent Mo layers are antiferromagnetically (AFM) ordered at T_N ranging from 13–26 K. For R = Gd, the sample is not SC and exhibit two magnetic transitions at 11 and 184 K. Both the SC or AFM states depend strongly on the R/Ce ratio and for R/Ce = 1, both states are suppressed.

DOI: 10.1103/PhysRevB.68.064507 PACS number(s): 74.25.Ha, 75.70.Cn

I. INTRODUCTION

Superconductivity (SC) and ferromagnetism (FM) are generally believed to be mutually antagonistic states. Coexistence of weak ferromagnetism (WFM) and SC was discovered a few years ago in $RuSr_2R_{2-x}Ce_xCu_2O_{10}$ (R = Eu and Gd, Ru-1222) layered cuprate systems,[1,2] and more recently[3] in $RuSr_2GdCu_2O_8$ (Ru-1212). The SC charge carriers originate from the CuO_2 planes and the WFM state is confined to the Ru layers. In both systems, the states *coexist* intrinsically on the microscopic scale. The Ru-1222 materials display a magnetic transition at $T_M = 125-180$ K and bulk SC below $T_c = 32-50$ K ($T_M > T_c$) depending on oxygen concentrations and sample preparation.[1] The hole doping of the Cu-O planes can be optimized with appropriate variation of the R/Ce ratio.[4] X-ray-absorption spectroscopy reveals that the Ru ions are Ru^{5+} irrespective of the Ce concentration.[5] The magnetic state of the Ru sublattice is not affected by the presence or absence the SC state, indicating that the two states are practically decoupled.[6] It is also apparent that bulk SC *only* appears in the M-1222 (M = Nb and Ta) with $T_c \sim 28-30$ K, in which the M ions are pentavalent.[7]

During the course of studying the Ru-1222 system, we noticed that Ru can be replaced completely by Mo ions and that the $MoSr_2R_{1.5}Ce_{0.5}Cu_2O_{10}$ (Mo-1222) system is isostructural to the Ru-1222 one. The Mo-1222 system can be obtained with most of the R elements (Pr-Yb and Y). In contrast to the M-1222 (M = Nb, Ta) systems, which are SC only and to the Ru-1222 materials, described above, in Mo-1222, the SC and the magnetic states compete with each other. Materials, which are SC, are not antiferromagnetic AFM, and vice versa. The ionic radii of the R ions determine whether the material is paramagnetic (PM), SC or AFM ordered. We show here that in Mo-1222: (i) the light R element (Pr and Nd) are PM. (ii) the middle R = Sm and Eu samples are SC at $T_c = 18-23$ K, and (iii) that the heavy R ions (Ho-Yb and Y) are AFM ordered with $T_N = 13-26$ K. We also present the magnetic curves of $MoSr_2Gd_{1.5}Ce_{0.5}Cu_2O_{10}$ in which we show two magnetic transitions at 11 and 184 K, and construct the SC-AFM phase diagram in Mo-1222.

II. EXPERIMENTAL DETAILS

Ceramic samples with nominal composition $MoSr_2R_{1.5}Ce_{0.5}Cu_2O_{10}$ (Mo-1222R) and $MoSr_2RCeCu_2O_{10}$ (R/Ce = 1) were prepared by a solid-state reaction technique. Prescribed amounts of R_2O_3, CeO_2, $SrCO_3$, Mo, and CuO were mixed and pressed into pellets and preheated at 950 °C for 1 day. The products were cooled, reground, and sintered at 1050 °C for 2 days under oxygen atmosphere and then furnace cooled. Part of the asp Mo-1222R (R = Eu, Gd, and Y) samples were re-heated for 12 h at 800 °C under high oxygen pressure (70 atm).

Powder x-ray-diffraction (XRD) measurements indicate that all samples are nearly single phase (~96%) materials and confirmed the tetragonal structure. The XRD patterns contain a few minor additional peaks and all attempts to completely get rid of them were unsuccessful. For the R = La and Lu samples, the extra peak intensity exceed 25%, therefore their lattice parameters are not listed. Within the instrumental accuracy, the lattice parameters of R/Ce = 1 samples are similar to the corresponding Mo-1222R compounds. The microstructure and the phase integrity of the materials were investigated by QUANTA (Fri Company) scanning electron microscopy (SEM) and by a Genesis energy dispersive x-ray analysis (EDAX) device attached to the SEM. Zero-field-cooled (ZFC) and field-cooled (FC) dc and ac magnetic measurements in the range of 2–400 K were performed as described in Ref. 4.

TABLE I. Lattice parameters and magnetic parameters of $MoSr_2R_{1.5}Ce_{0.5}Cu_2O_{10}$ (ND=not determined).

R	a (Å)	c (Å)	T_c/T_N (K)	C (emu K/mol Oe)	θ (K)	$10^3\chi_0$ (emu/mol Oe)	P_{eff} (μ_B)
Pr	3.861(1)	28.38(1)	PM	1.51(2)	−14.1(2)	1.1(1)	2.85
Nd	3.860	28.52	PM	1.00	−2.1	4.5	2.31
Sm	3.848	28.43	$T_c=18(1)$	0.12	−12.4	1.91	0.80
Eu	3.838	28.41	$T_c=23(1)$	not CW			
Gd	3.833	28.43	15, 184	9.6	14.7	3.0	7.16
Tb	3.818	28.33	ND	14.2	−8.5	3.0	8.70
Dy	3.815	28.37	ND	19.4	−4.9	11.0	10.1
Ho	3.812	28.40	13(1)	21.4	−4.4	4.7	10.6
Er	3.810	28.44	26	19.6	−11.3	0.1	10.1
Tm	3.797	28.30	13	10.7	−22.0	1.84	7.56
Yb	3.807	28.41	16	2.38	−7.5	2.2	3.58
Y	3.812	28.43	13	0.35	−1.4	0.5	1.68

III. EXPERIMENTAL RESULTS AND DISCUSSION

Least-squares fits of the XRD patterns of the $MoSr_2R_{1.5}Ce_{0.5}Cu_2O_{10}$ compounds on the basis of a tetragonal structure (SG $I4/mmm$) left a few minor reflections most of them belonging to R_2O_3 and to the $SrMoO_4$ phase and yield the lattice parameters given in Table I. The variation of the a lattice constant shown in Fig. 1, is attributed to the lanthanide contraction of the R^{3+} ions. The c constant can be considered as remaining constant. The similarity of a for R=Pr and Nd and the excess of a for R=Yb (Fig. 2) are most probably due to the mixed valence states of Pr and Yb. The morphology detected by the SEM shows a smooth and uniform surface for the granular the Mo-1222Eu sample, with typical grain size of 2–3 μm. For Mo-1222Y the grain size is not well defined. EDAX analysis confirms the initial stoichiometric composition of R:Ce:Sr and Cu, whereas a deficiency in the Mo content is obtained due to its volatility. We also detected a few separate sphere grains of the $SrMoO_4$ phase.

A. Paramagnetism in $MoSr_2R_{1.5}Ce_{0.5}Cu_2O_{10}$ (R=Pr and Nd)

The dc magnetic susceptibility $\chi(T)$ [$=M(T)/H$] curves of Mo-1222R (R=Pr, Nd, and La), exhibit normal PM behavior down to 5 K and the isothermal $M(H)$ (up to 5 T) curves are linear. The $\chi(T)$ curves can be fitted by the Curie-Weiss (CW) law: $\chi=\chi_0+C/(T-\theta)$, where χ_0 is the temperature-independent part of χ, C is the Curie constant, and θ is the CW temperature. $SrMoO_4$ detected by EDAX is Pauli paramagnetic[8] and does not contribute to C. In order to get the net R contribution to $\chi(T)$, we measured the $\chi(T)$ of Mo-1222Y (see below) and $\chi(T)$ of $YBa_2Cu_2O_7$ (at $T>100$ K) which is roughly temperature independent ($1.8-2\times10^{-4}$ emu/mol Oe). After subtracting the two contributions [$\frac{2}{3}\chi(T)$ of Y123] from the measured $\chi(T)$, we obtained χ_0, C, and the P_{eff} values listed in Table I. (The same procedure was done for all C values given in Table I.) For the PM Mo-1222R (R=Pr and Nd) materials, the extracted $P_{\text{eff}}=2.85$ and $2.31\mu_B$, respectively, are lower than the 3.56 and $3.62\mu_B$ expected for Pr^{3+} and Nd^{3+}. This re-

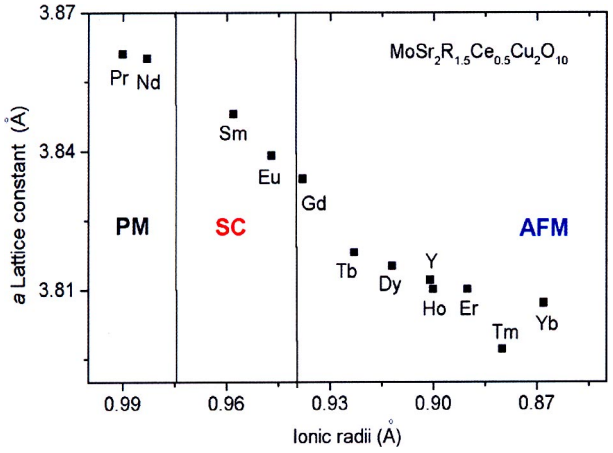

FIG. 1. (Color online) The phase diagram and the a lattice parameter as a function of the ionic radii in Mo-1222.

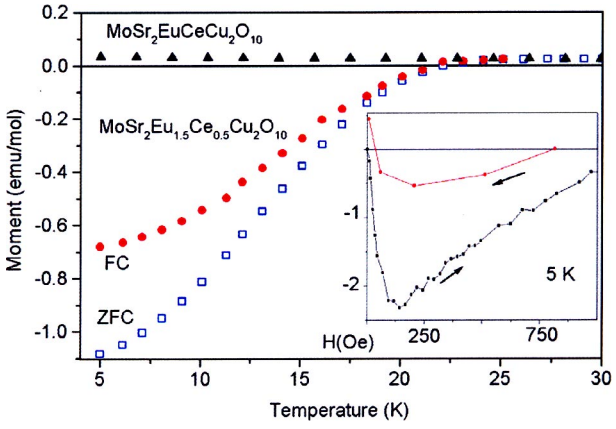

FIG. 2. (Color online) Magnetic moment of $MoSr_2Eu_{1.5}Ce_{0.5}Cu_2O_{10}$ (SC) and $MoSr_2EuCeCu_2O_{10}$ measured at 3 Oe. The inset shows the hysteresis loop at 5 for the SC material.

duction is probably due to strong crystal-field effects and/or to a mixed valence state of Pr as stated above. Note the difference between the two negative θ values of the materials.

B. Superconductivity in the $MoSr_2R_{1.5}Ce_{0.5}Cu_2O_{10}$ (R=Sm and Eu)

ZFC and FC magnetic curves for Mo-1222Eu are presented in Fig. 2. The onset of SC at $T_c=23$ K was also obtained by ac measurements. Annealing under high oxygen pressure did not change the T_c value. On the other hand, increasing the Ce concentration suppresses SC and $MoSr_2EuCeCu_2O_{10}$ is PM down to 5 K (Fig. 2). For R =Sm, $T_c=18$ is obtained. Above T_c, for R=Sm, the $\chi(T)$ plot follows the CW law (Table I), whereas, for R=Eu, the $\chi(T)$ curve is linear and does not obey the CW law.

With the purpose of acquiring information about the critical current density J_C, we have measured at 5 K the magnetic hysteresis (Fig. 2). Following the Bean's approach $J_C(H)=30\Delta M/d$, where ΔM is the difference in the M at the same H, and $d=2.5\,\mu$m, we obtained: $J_C=4.4\times10^4$ A/cm^2 (at $H=0$) a value which compares well with J_C obtained in Ru-1222 under the same conditions.[9]

Our intuitive explanation as to why all the M-1222 materials (M^{5+}) are SC is discussed in Ref. 4. Assuming that Mo is pentavalent, we may apply the same model to the Mo-1222 materials. In the well-established phase diagram for $La_{2-x}Sr_xCuO_4$, the parent La_2CuO_4 is AFM and insulating and replacing Sr^{2+} for La^{3+} varies the hole density p. In Mo-1222 (Sr^{2+}, Cu^{2+}, and O^{2-}), Ce is tetravalent[5] and our Mossbauer spectroscopy (MS) study performed at room temperature on ^{151}Eu shows a singlet with an isomer shift of 0.04(2) mm/s (relative to Eu_2O_3), indicating that the Eu is trivalent ($J=0$). This is consistent with the lattice parameter presented in Fig. 1 and Table I. Given that Mo is pentavalent, a straightforward valence count yields a fixed oxygen concentration of 10. Thus we argue that the $MoSr_2EuCeCu_2O_{10}$ sample serves as the parent compounds (similar to La_2CuO_4). Hole doping of the Cu-O planes, which results in SC, can be achieved with increasing of the R^{3+}/Ce^{4+} ratio (R^{3+} ions are replaced for Ce^{4+}) and indeed, $MoEu_{1.5}Ce_{0.5}Sr_2Cu_2O_{10-\delta}$ is SC. The optimal doping of Ce is now under investigation.

C. Antiferromagnetism in the $MoSr_2R_{1.5}Ce_{0.5}Cu_2O_{10}$ (R=Ho-Lu and Y)

The ZFC and FC curves of Mo-1222R (R=Y, Er, and Tm) measured at 5–10 Oe, are presented in Fig. 3. One definitely sees the irreversibility and the peaks in the ZFC plots, typical of canted AFM ordering. We define T_N (Table I) as the merging point of these branches or, alternatively, as the inflection point in the $d\chi(T)/dT$ of the FC curve. Similar behavior was observed for R=Ho and Lu. For R=Yb, no irreversibility is obtained and $T_N=16$ K was defined as the kink observed in both ZFC and FC curves. All $M(H)$ curves measured below and above T_N are linear up to 5 T and no hysteresis is observed.

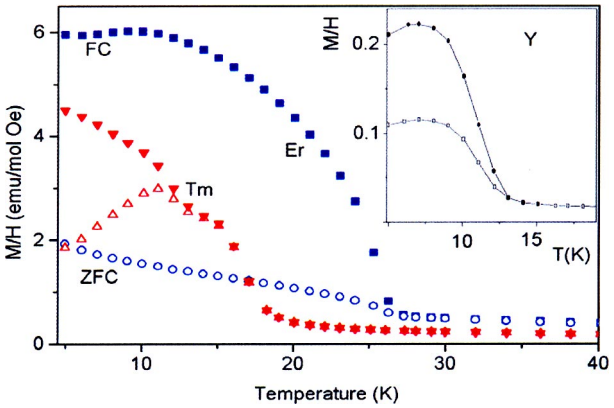

FIG. 3. (Color online) ZFC and FC susceptibility curves measured at low applied fields of Mo-1222R, R=Er, Tm, and Y (inset).

Above T_N, the $\chi(T)$ curve for Mo-1222Y follows the CW law, and provides useful information on the Mo valence. Taking into account the existence (of about 5–6%) of the $SrMoO_4$ phase and by subtracting the Cu contribution (see above) we obtained $P_{\rm eff}=1.68\mu_B$ a value which is in good agreement with $1.73\mu_B$ expected for Mo^{5+} ($4d^1$, $S=0.5$). Therefore we argue with high confidence that the prominent feature shown in Fig. 3, as well as the SC state described above, are related to the Mo^{5+} sublattice. This preferable interpretation, which invokes analogy to the Ru-1222 system, means that the Mo layers are AFM ordered at relatively low temperatures (13–26 K). The $P_{\rm eff}$ values for R =Ho-Yb (Table I) are in good agreement with their calculated R^{3+} free ion values. Note the negative θ obtained which is consistent with an AFM order.

For R=Tb and Dy, the $\chi(T)$ curves have a PM-like behavior down to 5 K. For R=Dy, the small contribution of the Mo AFM signal (0.2 emu/mol Oe for R=Y see Fig. 3 inset) is probably masked by the high PM susceptibility of Dy^{3+}. The $P_{\rm eff}$ value obtained (after subtracting the Mo contribution) fits well the expected value of Dy^3. For R=Tb, $P_{\rm eff}=8.7\mu_B$ deduced, is smaller than the $9.72\mu_B$ expected for free ion Tb^{3+}, probably due to strong crystal-field effects as discussed above.

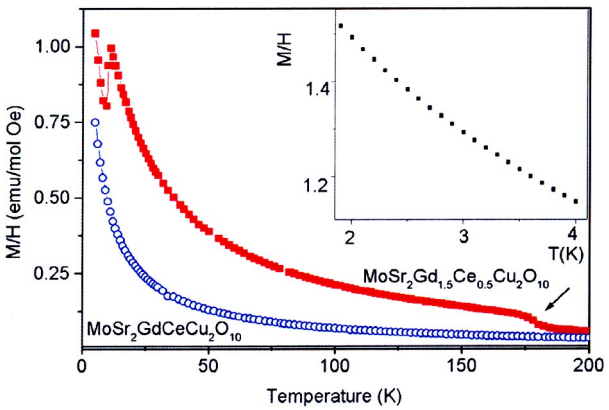

FIG. 4. (Color online) M/H of $MoSr_2Gd_{1.5}Ce_{0.5}Cu_2O_{10}$ and $MoSr_2GdCeCu_2O_{10}$ measured at 20 Oe. The inset shows the M/H curve for $MoSr_2Gd_{1.5}Ce_{0.5}Cu_2O_{10}$ at $T<4$ K.

D. $MoSr_2Gd_{1.5}Ce_{0.5}Cu_2O_{10}$ sample

This sample shows two magnetic transitions at 11 K and at 184 K and positive θ (Fig. 4). The $M(H)$ curves are linear and no hysteresis is observed. At 5 K, for $H>3$ T a tendency toward PM saturation (of Gd ions) is obtained. No magnetic transition is observed down to 1.8 K (Fig. 4 inset). This is in contrast to Gd123, *M*-1212 (M=Ru and Mo), and Ru-1222 in which Gd is AFM ordered at 2.2–2.6 K. (i) We may suggest that the peak at 11 K is related to the Gd sublattice and the highest transition is due to the Mo layers. (ii) A more preferable interpretation is that both transitions are related to the Mo sublattice, whereas the origin of the second one is not known yet. Our supporting evidence is the fact, that both magnetic transitions are very sensitive to the Gd/Ce ratio. For the Gd/Ce ratio <1.4 as well as in $MoSr_2GdCeCu_2O_{10}$ (Gd/Ce=1) both anomalies are absent (Fig. 4), suggesting that the two magnetic transitions are connected to each other. The PM values extracted for $MoSr_2GdCeCu_2O_{10}$ are: $\theta=-4.4$ K and $P_{\text{eff}}=7.85\mu_B$/Gd which fits well the theoretical value of $7.94\mu_B$/Gd. At the present moment we cannot explain why the R=Gd sample behaves so differently from all the rest of the heavy Mo-1222*R* compounds.

IV. CONCLUSION

We demonstrate that the behavior of Mo-1222 system is entirely different from Ru^{5+}-1222 one. In Mo-1222 (Mo^{5+}), the physical state depends strongly on the ionic radii of the *R* ionst. For large *R* ions, the samples are PM (Fig. 1). Once the *a* lattice parameter is contracted, SC in the CuO_2 planes is induced at $T_c\sim 20$ K. Further contraction of *a* leads to an AFM order (at T_N 13–26 K) in the Mo-O layers and to suppression of SC. The SC and AFM (which compete each other) states depend on the *R*/Ce ratio and both disappear for *R*/Ce=1. The magnetic behavior of the Gd sample is different. Neutron diffraction as well as MS on ^{155}Gd studies are now being carried out to determine the magnetic structure of this system.

ACKNOWLEDGMENTS

We are grateful to Professor I. Nowik for the Mossbauer data and to Professor S. Reich for the low-temperature magnetic measurements. This research was supported by the Israel Academy of Science and Technology and by the Klachky Foundation for Superconductivity.

[1] I. Felner, U. Asaf, Y. Levi, and O. Millo, Phys. Rev. B **55**, R3374 (1997).
[2] Y. Y. Xue, D. H. Cao, B. Lorenz, and C. W. Chu, Phys. Rev. B **65**, 020511(R) (2002).
[3] C. Bernhard, J. L. Tallon, Ch. Niedermayer, Th. Blasius, A. Golnik, E. Brucher, R. K. Kremer, D. R. Noakes, C. E. Stronach, and E. J. Ansaldo, Phys. Rev. B **59**, 14 099 (1999).
[4] I. Felner, U. Asaf, and E. Galstyan, Phys. Rev. B **66**, 024503 (2002).
[5] G. V. M. Williams, L. Y. Jang, and R. S. Liu, Phys. Rev. B **65**, 064508 (2002).
[6] I. Felner and E. Galstyan, Physica C (to be published).
[7] R. J. Cava, J. J. Krajewski, H. Takagi, H. W. Zandbergen, R. B. Van Dover, W. F. Peck, Jr., and B. Hessen, Physica C **191**, 237 (1992).
[8] S. I. Ikeda and N. Shirakawa, Physica C **341–348**, 785 (2000).
[9] I. Felner, E. Galstyan, B. Lorenz, D. Cao, Y. S. Wang, Y. Y. Xue, and C. W. Chu, Phys. Rev. B **67**, 134506 (2003).